

Photoproduction of π^0 on Protons by Polarized γ Rays

G. BARBIELLINI, G. BOLOGNA, G. CAPON, G. DE ZORZI, F. L. FABBRI, AND G. P. MURTAS
Laboratori Nazionali del CNEN, Frascati, Roma, Italy

AND

G. DIAMBRINI AND G. SETTE
Istituto di Fisica dell'Università di Genova and Istituto Nazionale di Fisica Nucleare, Genova, Italy

AND

J. DE WIRE
Cornell University, Ithaca, New York 14850
 (Received 10 March 1969)

The asymmetry $\Sigma(k, \theta^*) = (d\sigma_{\perp} - d\sigma_{\parallel}) / (d\sigma_{\perp} + d\sigma_{\parallel})$ of the polarized cross sections for π^0 photoproduction has been measured at $\theta^* = 90^\circ$ for energies k of the incident photon in the range 230–380 MeV. The experiment has been performed with the polarized γ -ray beam of the Frascati 1-GeV electron synchrotron. The experimental results are compared with the present theoretical predictions in order to investigate the importance of ω exchange in the t channel and the contribution of the $E_{1+}^{(3)}$ multipole at the 33 resonance. The theory with ω exchange is in the best agreement with the experiment.

I. INTRODUCTION

THE photoproduction of π^0 mesons has been extensively investigated both theoretically and experimentally in the past few years. A comprehensive reference index can be found in Beale *et al.*¹ In the present experiment the asymmetry of the cross sections from polarized photons for π^0 photoproduction on hydrogen ($\gamma p \rightarrow \pi^0 p$) has been measured using the coherent bremsstrahlung beam from a diamond. This beam is a Frascati electron-synchrotron facility.² The asymmetry has been measured at a proton angle of 90° in the c.m. system for photon energies in the range 230–380 MeV.

The experimental data have been collected in two periods, with slightly different experimental setups in each period. (In the following we will refer to them as experiments 1 and 2.) Preliminary results have been presented previously,³ but the evaluation of the polarization of the coherent γ -ray beam has now been improved.⁴ In this paper we give both the old and the new data on the asymmetry, all evaluated with the new, more accurate polarization values.

Linearly polarized bremsstrahlung has been used previously to investigate π^0 photoproduction by Drickey and Mozley.⁵ In their experiment polarized γ rays were obtained by selecting a small cone of the bremsstrahlung beam from a thin radiator at the Stanford Linear Accelerator, Mark III.

¹ J. T. Beale, S. D. Ecklund, and R. L. Walker, Report No. CTSL-42, CALT 68/108, 1968 (unpublished).

² G. Barbiellini, G. Bologna, G. Diambri, and G. P. Murtas, Phys. Rev. Letters **8**, 112 (1962).

³ G. Barbiellini, G. Bologna, J. De Wire, G. Diambri, G. P. Murtas, and G. Sette, in *Proceedings of the Twelfth Annual Conference on High-Energy Physics, Dubna, 1964* (Atomizdat, Moscow, 1965), p. 838; G. Barbiellini, G. Capon, G. De Zorzi, F. L. Fabbri, and G. P. Murtas, Contribution to the Heidelberg International Conference on Elementary Particles, 1967 (unpublished).

⁴ G. Barbiellini, G. Bologna, G. Diambri, and G. P. Murtas (unpublished).

⁵ D. J. Drickey and R. F. Mozley, Phys. Rev. **136**, B543 (1964).

II. NOTATION AND THEORETICAL SUMMARY

The differential cross section for π^0 photoproduction by linearly polarized photons is

$$\frac{d\sigma}{d\Omega}(k, \theta^*, \varphi) = \left[\frac{d\sigma}{d\Omega}(k, \theta^*) \right]_{\text{unpol}} + \frac{q}{k} I(k, \theta^*) \sin^2 \theta^* \cos 2\varphi, \quad (1)$$

where, in the c.m. system, k is the photon energy, q is the pion momentum, θ^* is the proton production angle, and φ is the angle between the photon-polarization plane and the production plane. Here $(d\sigma/d\Omega)_{\text{unpol}}$ is the π^0 photoproduction cross section for unpolarized photons. In terms of the usual Pauli⁶ amplitudes \mathcal{F}_i , the above functions are

$$\begin{aligned} k \left[\frac{d\sigma}{d\Omega}(k, \theta^*) \right]_{\text{unpol}} &= |\mathcal{F}_1|^2 + |\mathcal{F}_2|^2 - 2 \cos \theta^* \\ &\quad \times \text{Re} \mathcal{F}_1^* \mathcal{F}_2 + \sin^2 \theta^* I(k, \theta^*), \quad (2) \\ I(k, \theta^*) &= \frac{1}{2} |\mathcal{F}_3|^2 + \frac{1}{2} |\mathcal{F}_4|^2 + \cos \theta^* \text{Re} \mathcal{F}_3^* \mathcal{F}_4 \\ &\quad + \text{Re}(\mathcal{F}_1^* \mathcal{F}_4 + \mathcal{F}_2^* \mathcal{F}_3). \end{aligned}$$

The \mathcal{F}_i are, in general, complicated functions of $\cos \theta^*$ and of the photoproduction multipole amplitudes E_{l^*} and M_{l^*} . However, including only s and p waves, as seems reasonable in the region of the first pion-nucleon resonance, they are simplified considerably and are given by

$$\begin{aligned} \mathcal{F}_1 &= E_{0+} + 3 \cos \theta^* (E_{1+} + M_{1+}), \\ \mathcal{F}_2 &= 2M_{1+} + M_{1-}, \\ \mathcal{F}_3 &= 3(E_{1+} - M_{1+}), \\ \mathcal{F}_4 &= 0. \end{aligned}$$

Since this paper is concerned with the cross sections obtained by use of linearly polarized photons, we will

⁶ F. A. Berends, A. Donnachie, and D. L. Weaver, Nucl. Phys. **B5**, 1 (1967); **B5**, 54 (1967); **B5**, 103 (1967), hereafter referred to as BDW.

concentrate on the information obtainable in such experiments.

For experimental purposes we write Eq. (2) as

$$\frac{k}{q} \left[\frac{d\sigma}{d\Omega}(k, \theta^*) \right]_{\text{unpol}} = A + B \cos\theta^* + C \cos^2\theta^* + \dots,$$

where, neglecting d and higher partial waves, we obtain

$$\begin{aligned} A &= |E_{0+}|^2 + \frac{5}{2} |M_{1+}|^2 + |M_{1-}|^2 + \frac{9}{2} |E_{1+}|^2 \\ &\quad + \text{Re}[M_{1+}^*(M_{1-} - 3E_{1+}) + 3M_{1-}^*E_{1+}], \\ B &= 2 \text{Re}[E_{0+}^*(3E_{1+} + M_{1+} - M_{1-})], \\ C &= \frac{9}{2} |E_{1+}|^2 - \frac{3}{2} |M_{1+}|^2 + 3 \text{Re}[M_{1+}^*(3E_{1+} - M_{1-}) \\ &\quad - 3E_{1+}^*M_{1-}]. \end{aligned}$$

We have, also,

$$I(k, \theta^*) = I_0 + I_1 \cos\theta^* + \dots,$$

where, in the s - and p -wave approximation,

$$\begin{aligned} I_0 &= \frac{9}{2} |E_{1+}|^2 - \frac{3}{2} |M_{1+}|^2 \\ &\quad - 3 \text{Re}[M_{1+}^*(M_{1-} + E_{1+}) - E_{1+}^*M_{1-}], \end{aligned}$$

and where the higher terms are all zero. The asymmetry is defined by

$$\Sigma(k, \theta^*) = \frac{d\sigma_1(k, \theta^*) - d\sigma_{11}(k, \theta^*)}{d\sigma_1(k, \theta^*) + d\sigma_{11}(k, \theta^*)},$$

where $d\sigma_{1,11}(k, \theta^*)$ are the π^0 photoproduction cross sections for photons with polarization vectors, respectively, normal or parallel to the production plane. This expression for $\Sigma(k, \theta^*)$ may be written

$$\Sigma(k, \theta^*) = -\sin^2\theta^* I(k, \theta^*) / \left[\frac{k}{q} \left[\frac{d\sigma}{d\Omega}(k, \theta^*) \right]_{\text{unpol}} \right].$$

One sees that, in fact, $I(k, \theta^*)$ is independent of θ^* in the s - and p -wave approximation, so that measurement of this quantity away from $\theta^* = 90^\circ$ gives a test of the approximation [an angular distribution of $I(k, \theta^*)$ deviating from a constant would indicate that higher partial waves are needed].

Another quantity of interest is I_0/C , which, in the s - and p -wave approximation, has the form

$$\frac{I_0}{C} = \frac{\frac{9}{2} |E_{1+}|^2 - \frac{3}{2} |M_{1+}|^2 - 3 \text{Re}[M_{1+}^*(M_{1-} + E_{1+}) - E_{1+}^*M_{1-}]}{\frac{9}{2} |E_{1+}|^2 - \frac{3}{2} |M_{1+}|^2 + 3 \text{Re}[M_{1+}^*(3E_{1+} - M_{1-}) - 3E_{1+}^*M_{1-}]}. \quad (3)$$

If $E_{1+} = 0$ then $I_0/C = 1$, so that this quantity is sensitive to small values of E_{1+}/M_{1+} , a quantity of interest as a test of symmetry schemes. For example, in the non-relativistic quark model, Becchi and Morpurgo⁷ show that the electric quadrupole amplitude to the P_{33} final state $E_{1+}^{(3)}$ must be identically zero at the resonance position. Of course, at the first resonance there are also nonresonant contributions to E_{1+} , the isospin structure being

$$E_{1+}^{\pi^0 p} = E_{1+}^{(0)} + \frac{1}{3} E_{1+}^{(1)} + \frac{2}{3} E_{1+}^{(3)}$$

in the usual notation. In fact, using the theoretical results of Berends *et al.*,⁶ $E_{1+}^{(0)} + \frac{1}{3} E_{1+}^{(1)}$ is fairly energy-independent around the resonance position and has a magnitude (at 340-MeV photon lab energy)

$$\begin{aligned} \text{Re}(E_{1+}^{(0)} + \frac{1}{3} E_{1+}^{(1)}) &= 1.31 \times 10^{-3}, \\ \text{Im}(E_{1+}^{(0)} + \frac{1}{3} E_{1+}^{(1)}) &= 0.04 \times 10^{-3}. \end{aligned}$$

Here the units are $\hbar = c = \mu = 1$. At the same energy, one has

$$\begin{aligned} \text{Re}M_{1+}^{\pi^0 p} &= 0.6 \times 10^{-3}, & \text{Im}M_{1+}^{\pi^0 p} &= 24.4 \times 10^{-3}, \\ \text{Re}M_{1-}^{\pi^0 p} &= -5.53 \times 10^{-3}, & \text{Im}M_{1-}^{\pi^0 p} &= 0.55 \times 10^{-3}. \end{aligned}$$

These values indicate that the interference terms in Eq. (3) are not negligible compared with $|M_{1+}^{\pi^0 p}|^2$, and so I_0/C may differ significantly from unity without invalidating the quark model in any way.

Therefore, from the measurement of I_0/C one cannot directly infer whether $E_{1+}^{(3)}$ is equal to or different from

⁷ C. Becchi and G. Morpurgo, Phys. Letters **17**, 352 (1965).

zero. The correct procedure is to rely on a set of multipoles given by the theorists and then to compare the theoretical values of I_0/C (obtained with and without the position $E_{1+}^{(3)} = 0$) with the experimental value.

The quantity I_0 can also be used to gain information about the multipole M_{1-} . If the s - and p -wave approximation is valid, and if one takes the E_{1+} and M_{1+} multipoles as given by theory, then the measurement of I_0 in π^0 photoproduction from protons can be combined with the recent measurement of the asymmetry of π^- photoproduction from neutrons⁸ to obtain an estimate of the multipoles $M_{1-}^{(0)}$ and $M_{1-}^{(1)}$. The isospin combinations are

$$\begin{aligned} M_{1-}^{\pi^0 p} &= M_{1-}^{(0)} + \frac{1}{3} M_{1-}^{(1)} + \frac{2}{3} M_{1-}^{(3)}, \\ M_{1-}^{\pi^- n} &= \sqrt{2} (M_{1-}^{(0)} - \frac{1}{3} M_{1-}^{(1)} + \frac{1}{3} M_{1-}^{(3)}), \end{aligned} \quad (4)$$

where $M_{1-}^{(0)}$ and $M_{1-}^{(1)}$ are the isospin $\frac{1}{2}$ multipoles for the P_{11} pion-nucleon final state, which contains the Roper resonance. The study of the $M_{1-}^{(0,1)}$ multipoles is important because their size bears on the existence of a $\{1\bar{0}\}$ SU_3 multiplet, as emphasized recently by Donnachie.⁹ $\gamma + p$ is a U -spin doublet ($U = \frac{1}{2}$) and $\gamma + n$ has $U = 1$. Since P_{11} in a $\{1\bar{0}\}$ has $U = 1$, photoproduction of P_{11} from protons is forbidden and photoproduction of P_{11} from neutrons is allowed by U -spin conservation.

This is one of the tests of the existence of a $\{1\bar{0}\}$

⁸ T. Nishikawa *et al.*, Phys. Rev. Letters **21**, 1288 (1968).

⁹ A. Donnachie, Phys. Letters **24B**, 420 (1967).

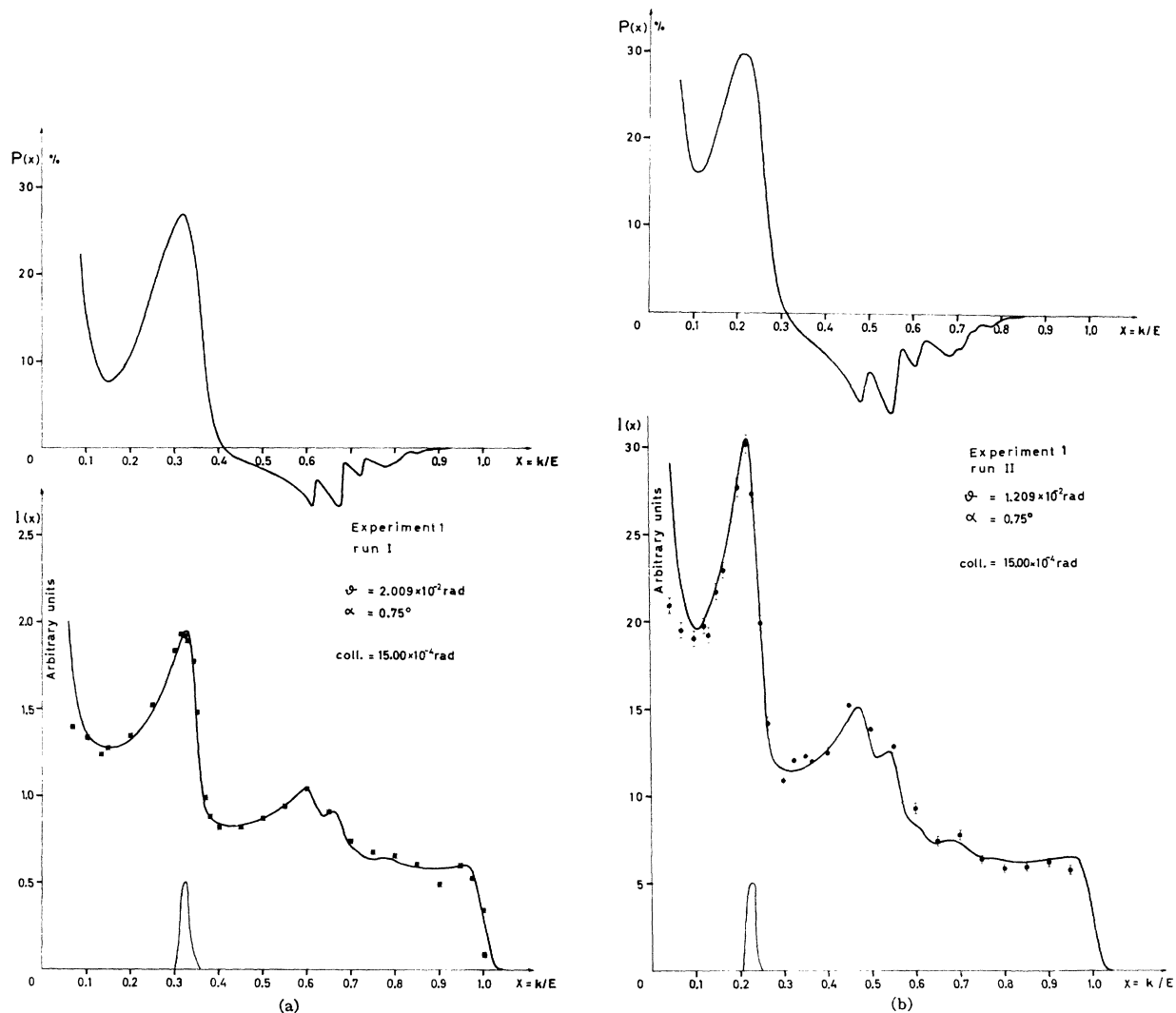


FIG. 1. Beam polarization and intensity versus the fractional photon energy $x = k/E$ for the different kinematical conditions. Full lines represent the calculated values. Experimental points refer to the measurements made with the electron-pair spectrometer. The bell-shaped curves along the x axis represent the energy acceptance of the experimental apparatus for π^0 photoproduction.

multiplet proposed by Lipkin.¹⁰ Recent theoretical investigations¹¹ have indicated that P_{11} photoproduction from neutrons would be greatly enhanced, thus favoring the existence of $\{1\bar{0}\}$. However, the experiment of Nishikawa *et al.* seems to indicate that P_{11} is not strongly produced in the reaction $\gamma + n \rightarrow \pi^- + p$. The quark model in its usual form does not permit the formation of a $\{1\bar{0}\}$, so it would be favored by this interpretation of the experiments. A theoretical estimate of $M_{1-}^{(0,1)}$ using partial-wave dispersion relations depends on an evaluation of the dispersion integral over the Roper resonance, which is highly inelastic; thus the Watson theorem does not apply, and the evaluation is very difficult.

¹⁰ H. J. Lipkin, Phys. Letters **12**, 154 (1964).

¹¹ W. Schmidt, in Proceedings of the Dubna Conference, 1967 (unpublished).

The best theoretical description of π^0 photoproduction available at present is based on partial-wave (multipole) dispersion relations.¹² In these, one projects out the multipoles from the fixed momentum-transfer dispersion relations for the 12 Chew-Goldberger-Low-Nambu invariant photoproduction amplitudes, including the isospin multiplicity, and then attempts to solve the resulting set of coupled integral equations using pion-nucleon phase shifts as input via the Watson theorem. Within these limitations there are, in addition, the following sources of error introduced in obtaining a solution to the dispersion relations.

¹² Most recent works on dispersion relations for pion photoproduction beyond the cited one by Berends *et al.* are D. Schwela, H. Rollnik, A. Weizel, and W. Korth, Z. Physik **202**, 452 (1967); W. Schmidt, Report No. SLAC-PUB-415, 1968 (unpublished); J. Engels, A. Müllensiefen, and W. Schmidt, Phys. Rev. **175**, 195 (1968).

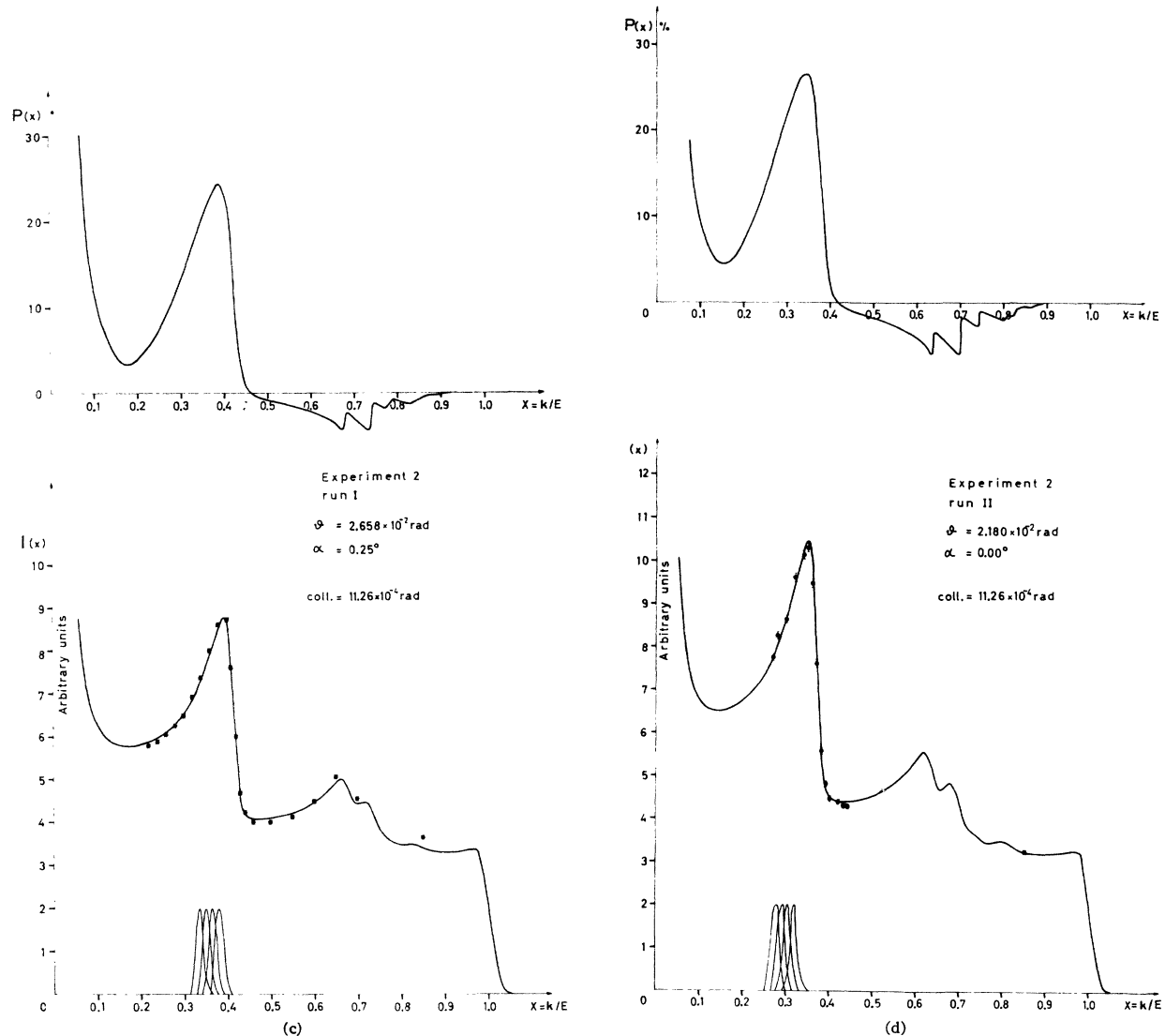


FIG. 1 (continued)

(1) Errors in the partial-wave Born terms due to the error in the coupling constant g .

(2) Errors introduced via the Watson theorem from the errors on the πN scattering phase shifts.

(3) Errors from the estimation of the rescattering contributions to the multipole $M_{1-}^{(0,1)}$ due to the P_{11} resonance, and to the multipoles $E_{2-}^{(0,1)}$, $M_{2-}^{(0,1)}$ due to the D_{13} resonance. These resonances are outside the region of validity of the Watson theorem for these particular partial waves but near enough to the energies of interest to affect the multipoles.

(4) Errors due to the unknown high-energy behavior of the multipoles.

We summarize the present theoretical situation by noting that theory (in its exclusion of parameters chosen to fit photoproduction data) inadequately

describes the experimental data. There are several problems which complicate the theoretical evaluation. The first is that in π^0 photoproduction on protons near threshold there is almost complete cancellation of what should nominally be the dominant terms, namely, the E_{0+} transitions to the s -wave final states. This leaves the cross section to be determined by the p waves, and near threshold the M_{1-} transition is as important as the M_{1+} . The second problem is that there should be some contribution from vector-meson exchange. This is indicated by the way in which Reggeized ω exchange can adequately explain high-energy π^0 photoproduction,¹³ especially if some background B exchange is included.¹⁴

¹³ H. P. Locher and H. Rollnik, Phys. Letters 22, 696 (1966).

¹⁴ J. P. Ader, M. Capdeville, and Ph. Salin, CERN Report No. TH-303, 1967 (unpublished).

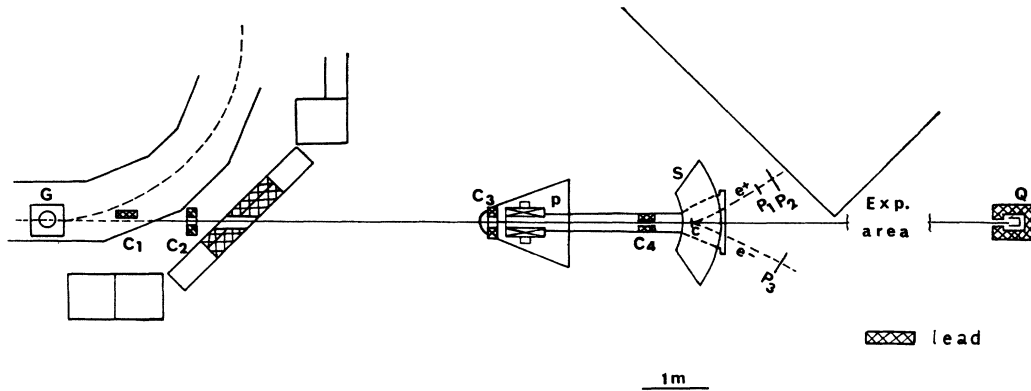


FIG. 2. General layout of the polarized beam. *G* is a goniometer holding the crystal diamond (installed inside the synchrotron vacuum chamber). *C*₁–*C*₄ are lead collimators. *P* is a broom magnet. *S* is an electron-pair spectrometer. *P*₁–*P*₃ are electron-pair counters. *Q* is a Wilson-type quantameter.

Including the vector mesons correctly is not easy because of the following.

(1) The vector-meson nucleon-coupling constants are not well known.¹⁵

(2) To be completely correct, one must include the effect of the vector-meson exchange on the entire multipole via the dispersion relation and not simply add the Born term.

(3) The effect of the vector-meson exchange may be already partially included in the final-state interactions introduced via the pion-nucleon phase shifts.¹⁶

These difficulties have been partially overcome by the introduction of several free parameters into the theory either correlated, as vector-meson parameters,⁶ or independent and representing the unknown high-energy behavior.^{16,17}

Finally, the calculation of the π^0 photoproduction cross sections by using the isobar model, originally due to Gourdin and Salin,¹⁸ has been refined recently by Walker.¹⁹

III. POLARIZED γ BEAM

The linearly polarized γ -ray beam used in the experiment is obtained from electron bremsstrahlung on a crystal diamond. The primary electrons are accelerated to 1000-MeV energy in the Frascati electron synchrotron. The properties of the coherent bremsstrahlung beam have been extensively described by Diambri-Palazzi.²⁰ A paper⁴ with more details on the calculation of the beam spectrum and polarization will be soon published. In the following paragraphs we briefly recall the employing features of the beam.

The diamond is oriented in such a way that the electron momentum \mathbf{p}_1 lies in the plane of the axes [110], [001] at a small angle θ with respect to the [110] axis.²¹ Then the γ -ray energy spectrum presents a

¹⁶ D. Schwela, Ph.D. thesis, Bonn University (unpublished).

¹⁷ H. Rollnik, in *Proceedings of the Heidelberg International Conference on Elementary Particles, 1967* (Wiley-Interscience, Inc., New York, 1968), p. 400; H. Rollnik, D. Schwela, and R. Werzley, contribution to the Heidelberg International Conference on Elementary Particles, 1967 (unpublished).

¹⁸ H. Gourdin and P. Salin, *Nuovo Cimento* **27**, 193 (1963).

¹⁹ R. L. Walker, Caltech Report No. CALT-158/68, 1968 (unpublished).

²⁰ G. Diambri-Palazzi, *Rev. Mod. Phys.* **40**, 611 (1968).

²¹ If α is the angle between the planes [110], [001], and \mathbf{p}_1 . [110], then under our nominal working conditions, α is 0° . The beam polarization is also dependent on α and has a relative maximum (keeping θ fixed) at $\alpha=0^\circ$. We estimate that the error on the polarization due to the misalignment on α is less than $\Delta P=0.01$.

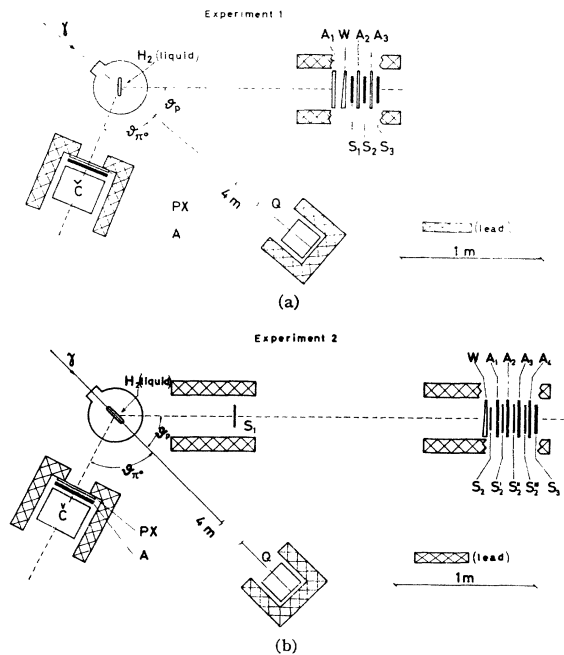


FIG. 3. Setup for experiments 1 and 2. *A*₁–*A*₄ and *W* are aluminum absorbers. *S*₁, *S*₂, *S*₂', *S*₂'', *S*₂'', *S*₃, and *A* are plastic scintillation counters. *C* is an integral lead-glass Čerenkov counter. *PX* is a Plexiglas layer (to stop slow electrons). The hydrogen target in experiment 1 is a disk 2.2 cm thick with axis parallel to the proton direction; in experiment 2 it is a cylinder along the beam direction of 15-cm length and 3-cm diam.

¹⁵ D. L. Weaver, *Phys. Letters* **26B**, 451 (1968).

ELECTRONICS BLOCK DIAGRAM (Experiment 2)

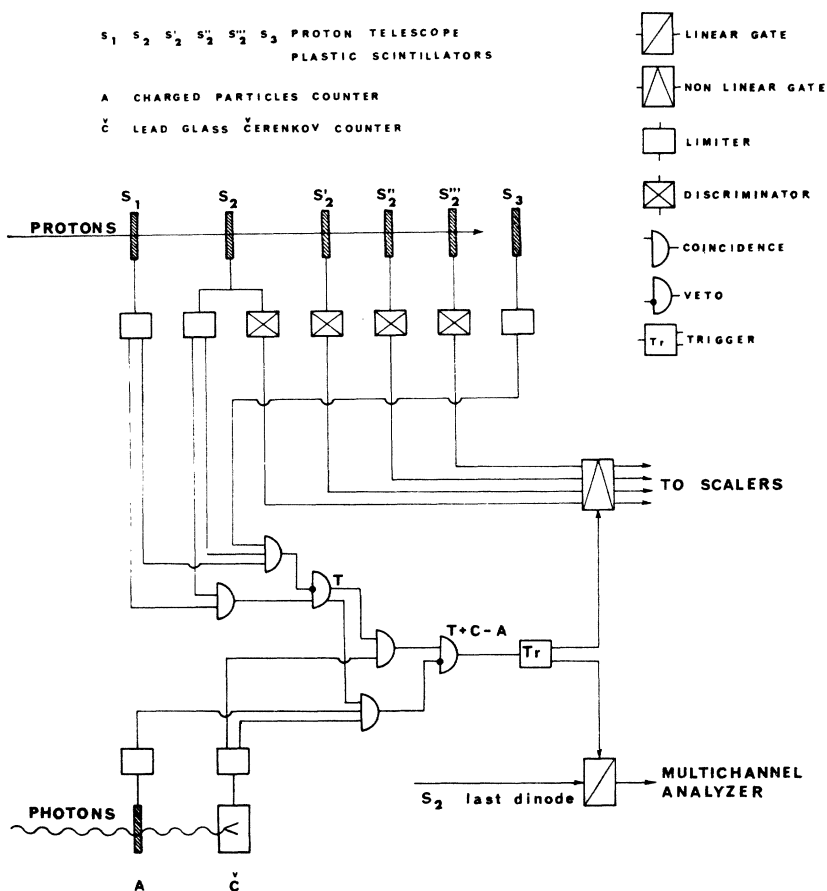


FIG. 4. Electronics block diagram (for experiment 2).

dominant peak of intensity, which corresponds to a maximum of the polarization P . The energy of the peak depends on the angle θ between \mathbf{p}_1 and the $[110]$ axis. The position of the peak can be chosen to obtain the largest number of useful photons in the required energy range. The polarization is defined as

$$P(k) = \frac{N_n(k) - N_p(k)}{N_n(k) + N_p(k)} = \frac{I_n(k) - I_p(k)}{I_n(k) + I_p(k)},$$

where k is the photon energy and $N_{n(p)}(k)$ is the number of photons per unit energy interval with electric vector normal (parallel) to the $[110]$ - $[001]$ plane, and where $I_{n(p)}(k) = kN_{n(p)}(k)$ is the bremsstrahlung intensity.

The experimental data are collected by using two diamonds: The plane $[110]$ - $[001]$ is vertical for the first one, horizontal for the second one. In the first (second) case we have an excess of photons with polarization vector parallel (normal) to the reaction plane which is horizontal in our experiment. Then, if C_1 and C_{11} are, respectively, the π^0 -photoproduction counting rates for the two situations at the same θ ,

one obtains the asymmetry of the cross sections via the formula²²

$$\Sigma = \frac{1}{|P|} \frac{R_c - 1}{R_c + 1}, \quad R_c = \frac{C_1}{C_{11}}.$$

During the experiment the beam energy spectrum has been measured with a pair spectrometer of energy resolution $\Delta k/k = \pm 4\%$.

The rotations of the diamond crystals are remotely controlled, and their values are read on two goniometers.

Figure 1 shows the measured spectra for the two diamonds corresponding to the θ values used in the experiment. The solid line represents the calculated spectrum. It is obtained from a computer program in which the interferential and amorphous bremsstrahlung cross sections are calculated and then folded with the experimental conditions, including electron scattering in the diamond, beam collimation, and finite energy resolution of the pair spectrometer. The normalization factor, the values of θ and α , and a parameter connected

²² J. De Wire, Frascati Report No. LNF-61/39, 1961 (unpublished).

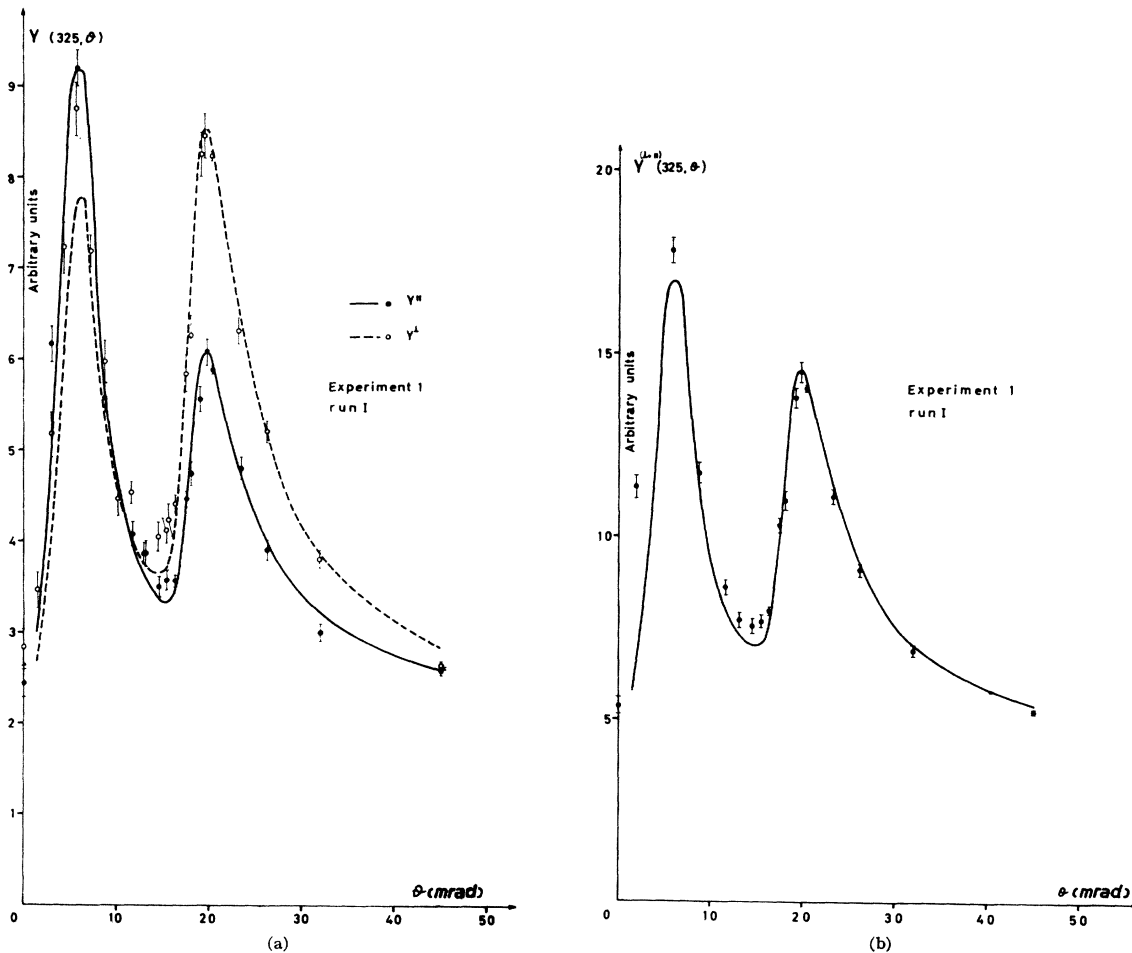


FIG. 5. Yield of photoproduction events versus the crystal angle θ for the different kinematical conditions. The solid and dashed curves represent, in arbitrary units, $Y_{\parallel}(\theta)$, $Y_{\perp}(\theta)$ and their sum calculated according to Eq. (5).

to the continuous part of the spectrum are left as free parameters. Their values are determined from the comparison with the measured spectrum by means of a least-squares method. The polarization $P(k)$ associated with this so-calculated intensity spectrum is assumed to be the true-beam polarization and is also shown in Fig. 1. The errors on the polarization values are due to the approximations still present in the calculation and to the statistical uncertainties in fitting the experimental spectrum. As a reasonable estimate from the least-squares analysis, we have assumed $\Delta P = 0.01$ as a standard error on the polarization. (For more details on the polarization calculation see Ref. 4).

The beam-experiment apparatus is shown in Fig. 2. Leaving the synchrotron doughnut, the γ -ray beam passes through collimators C_1 – C_4 . Its angular aperture is defined by C_3 , while C_1 has the function of eliminating the parasitic nonpolarized beam coming from the diamond holder; C_2 and C_4 reduce the background in the electron-pair spectrometer.

After the collimation, the beam enters the liquid-

hydrogen target H . P is a broom magnet and Q is a Wilson-type quantameter with the beam intensity monitored.

IV. EXPERIMENTAL APPARATUS

The π^0 photoproduction events are defined by a pulse coincidence between a proton-range telescope and

TABLE I. Kinematic conditions for the experimental runs. ϵ_{π^0} is the mean-geometrical Čerenkov efficiency for detecting a π^0 decay.

Expt. Run	k_0 (MeV)	θ_p (deg)	T_p (MeV)	θ_{π^0} (deg)	$\Delta\Omega_p$ (sr)	ϵ_{π^0}
1	I 325	40.5	61	73	0.0064	0.25
	II 230	35.6	28.5	74	0.0064	0.13
2	I 335	41	61	72	0.0036	0.13
	350	41	67	72	0.0036	0.14
	365	41	72	72	0.0036	0.155
	380	41	78	72	0.0036	0.165
	II 275	40	41.5	73	0.0036	0.15
	290	40	46.5	73	0.0036	0.17
	305	40	52.5	73	0.0036	0.18
	320	40	58	73	0.0036	0.20

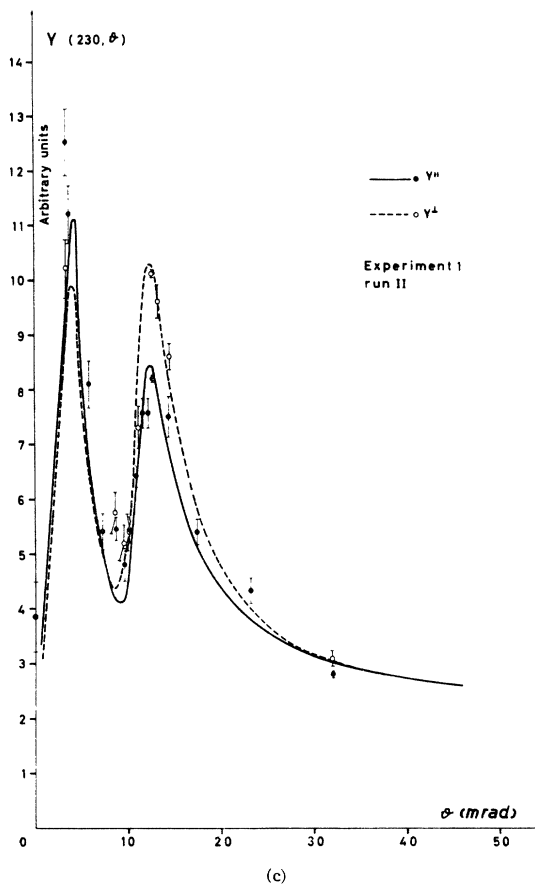
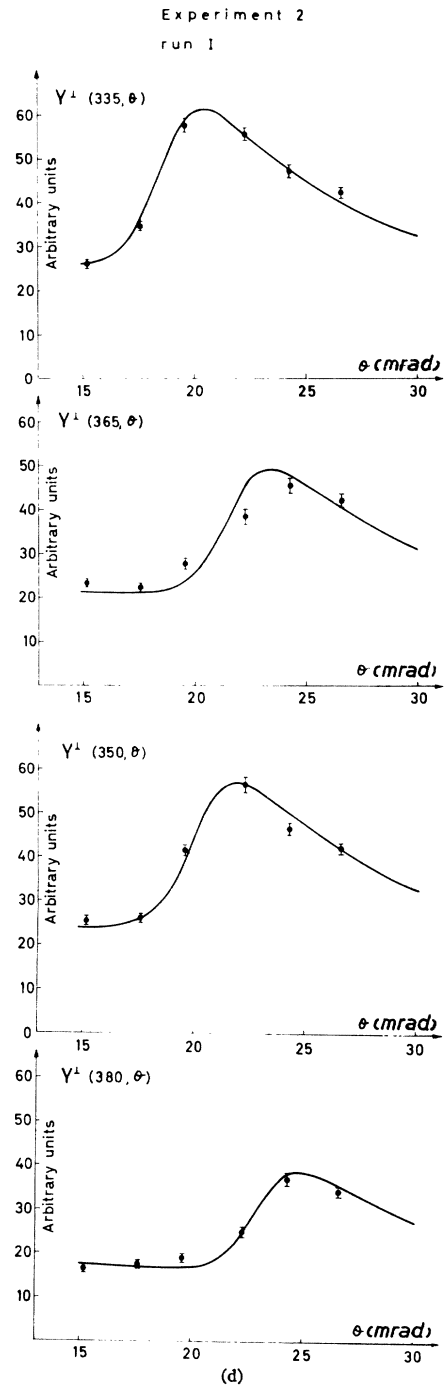


FIG. 5 (continued)



a lead-glass Čerenkov counter that detects one of the γ 's from the π^0 decay. A plastic scintillator *A* in front of the Čerenkov counter vetoes the detection of charged particles.

The proton-range telescope is an array of plastic scintillation counters and aluminum absorbers. In the first experiment, it defines only one energy channel. In the second one, three more counters and absorbers

have been added (see Fig. 3) in order to collect events simultaneously in four energy channels. The pulse height of the scintillation counter S_1 (S_2) in experiment 1 (2) is analyzed in a multichannel analyzer in order to control pion and electron contamination in the proton telescope. The central kinematic conditions for the two experiments are given in Table I.

In Fig. 4 is shown the electronic-block diagram for

experiment 2 (for experiment 1 the same logic has been used, but in a version simplified because of the absence of counters S_2' , S_2'' , S_2'''). Moreover, in experiment 2, discrimination between protons and pions also has been achieved by using their different time of flight, because of the increased distance between counters S_1 and S_2 .

The resolution power of the apparatus with respect to the initial photon energy k has been calculated for all kinematical conditions by a Monte Carlo method. In Fig. 1 the calculated resolution functions are shown: the typical total width at half-height is 20–30 MeV. Properly shaped absorbers have been used to obtain the form of the resolution function as square as possible.

The presence of steeply falling peaks in the beam spectrum allows us to calibrate the energy scale of our apparatus. By changing the crystal angle θ , it is possible to shift the coherent photon peak along the k axis. Then the π^0 photoproduction counting rate versus θ will have a relative maximum whenever a beam peak superimposes itself on the k -resolution curve of the experimental apparatus. The fit of the experimental data with the calculated predictions, obtained from the known photon-energy spectra shape gives the central energy value k_0 and the width of the resolution function.

The experimentally measured quantity is

$$Y_{\text{expt}}^{\perp, \parallel}(\theta) = C_{\perp, \parallel}(\theta) / N_e(\theta),$$

where $C_{\perp, \parallel}(\theta)$ are the π^0 photoproduction events per unit beam dose detected when the diamond is set at the angle θ and with the polarization, respectively, normal or parallel to the reaction plane, and where $N_e(\theta)$ is the number of the electron pairs, counted with the pair spectrometer per unit beam dose produced by 850-MeV photons when the diamond is set at the angle θ .²³

The calculated value $Y_c(\theta)$ to be compared to the experimental one is given by

$$Y_c^{\perp, \parallel}(\theta) = M \int \eta(k - k_0) n(\theta, k) \frac{d\sigma}{d\Omega}(k) \times [1 \pm \Sigma(k) P(\theta, k)] dk / [N_e(\theta)]_c, \quad (5)$$

where M is a normalization factor, $\eta(k - k_0)$ is the experimental apparatus-resolution function evaluated with the Monte Carlo method, k_0 is the nominal central-energy value, $n(\theta, k)$ is the calculated beam-energy spectrum at the crystal angle θ , and $P(\theta, k)$ is the corresponding beam polarization. Further, $d\sigma(k)/d\Omega$ is the π^0 photoproduction differential cross section at 90° in the c.m. system. The values used in the integral are the experimental data taken from Ref. 1. In addition, $\Sigma(k)$ is the π^0 photoproduction asymmetry previously defined. For our purposes, an accurate knowledge of $\Sigma(k)$ is not necessary; we have used the theoretical values given by Rollnik.¹⁹ Finally, $[N_e(\theta)]_c$

²³ For practical reasons (see also Ref. 4), it is more convenient to normalize the π^0 counting rates to the number of electron pairs rather than to the absolute beam dose.

TABLE II. Experimental results.

k_0 (MeV)	N	\bar{P}	R_c	$\Sigma(90^\circ)$	Expt.
325	60.000	0.262	1.371±0.011	0.596±0.028*	1
230	20.000	0.290	1.258±0.017	0.435±0.041	
275	16.800	0.185	1.196±0.018	0.485±0.049	2
290	31.800	0.210	1.284±0.014	0.592±0.039	
305	29.300	0.233	1.276±0.014	0.521±0.034	
320	34.300	0.252	1.408±0.015	0.672±0.034	
335	17.300	0.183	1.251±0.019	0.609±0.053	
350	15.300	0.204	1.297±0.020	0.634±0.050	
365	10.300	0.223	1.322±0.025	0.603±0.052	
380	11.200	0.236	1.319±0.024	0.583±0.047	

* The errors on the asymmetry have been calculated according to Eq. (6). However, for $\Sigma(230 \text{ MeV})$, which has a large background correction, we have included a systematic error equal to 20% of the calculated correction.

is the calculated value of the yield $N_e(\theta)$ of the electron pairs (see Ref. 20).

The experimental points with the corresponding calculated curves are shown in Fig. 5. The calculated curves have been optimized with the minimum χ^2 method with respect to the following parameters: (1) α (assumed to be the same for all the spectra with equal θ); (2) the percentage of the continuous (non-coherent) part in the beam spectrum; (3) the central value k_0 of the energy-resolution function and the normalization factor M .

The position of the last peak of the yield $Y(\theta)$ is very sensitive to the k_0 value. The comparison between experimental points and calculated prediction allows an evaluation of k_0 with an error of ± 5 MeV.

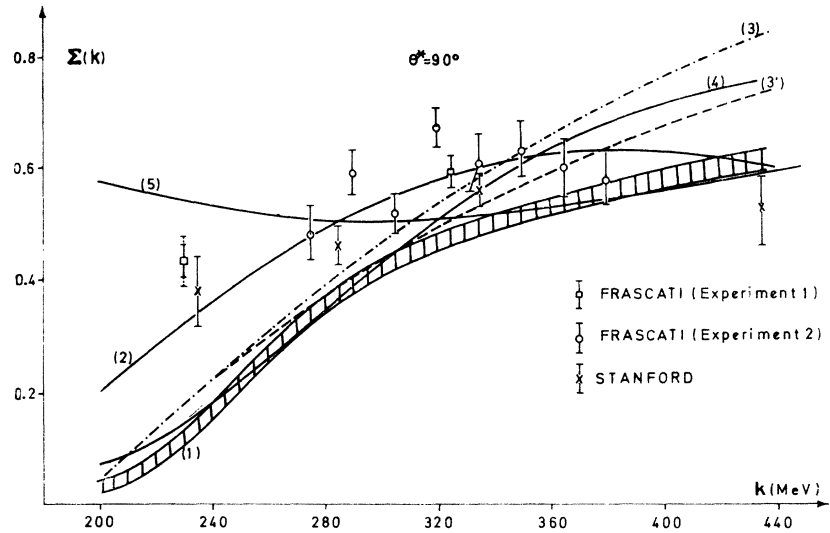
The agreement between the calculated curves and the experimental points is rather satisfactory. The deviations still existing can be attributed to (a) errors in the crystal-angle θ measurement; (b) contamination arising from the proton Compton effect. The number of events resulting from the Compton effect is on the average small (1–2%). However, the percentage of these events increases for some values of the crystal angle θ because of the different photon-energy regions contributing to π^0 photoproduction and Compton effect at the same proton kinematics; and (c) the approximations introduced in the photon-energy spectrum calculation start to fail at high values of the crystal angle θ . At these angles the calculation overestimates the photon intensity and consequently $Y_c(\theta)$.

V. EXPERIMENTAL RESULTS

The experimental values for the asymmetry are presented in Table II. N is the total number of π^0 photoproduction events. \bar{P} is the polarization value obtained by averaging $P(k)$ over the product of the k -resolving power, beam spectrum, and the differential π^0 production cross section. The values of \bar{P} are slightly different from the values of $P(k_0)$ corresponding to the center of the resolution curve.

The following concurrent reactions have to be considered.

FIG. 6. Asymmetry for π^0 photoproduction at $\theta^* = 90^\circ$. The Stanford points are taken from Ref. 5. Theoretical curves 1, 2, 3 and 3', 4, 5 are taken, respectively, from Refs. 6, 17, 16, 12, and 19.



(a) *Proton Compton effect.* The contamination introduced by the proton Compton effect is small, because the cross section for this process is nearly 1% of the π^0 corresponding cross section. We have not made corrections for this effect.

(b) *Double π^0 photoproduction.* The production of polarized photons with coherent bremsstrahlung requires that the maximum energy of the spectrum stays beyond the energy value of the useful polarized photons. Photons from the high-energy part of the spectrum (where the polarization is nearly zero) produce double π^0 photoproduction events which are seen by our apparatus. This background independent of the polarization has the effect of reducing the experimental ratio R_c and consequently introduces an underestimation of the asymmetry. Since precise experimental information on double π^0 photoproduction cross section is lacking, we have measured the contamination of this process in our experiment. This has been done only for the experimental situation corresponding to the photon energy $k_0 = 325$ MeV. This contamination is measured as the difference of the yields in our apparatus, per constant flux of 325-MeV photons, by setting the tip of an amorphous bremsstrahlung spectrum at 1000 and 500 MeV, respectively. In the second situation, all the photons are below our kinematical threshold for two- π^0 production. By taking into account the difference between the amorphous and the coherent bremsstrahlung spectrum, the measured double- π^0 contamination turns out to be 1.6% of the good events (after correction for nuclear absorption).

For the other kinematical conditions the double- π^0 contamination has been estimated from the previous one (measured at $k_0 = 325$ MeV) by correcting it for the following effects. (i) differences in the yields of photons contributing to single- and double- π^0 photoproduction; (ii) variation of the Čerenkov geometrical efficiency for

single- and double- π^0 production; and (iii) variation of the single- π^0 photoproduction cross section.

The energy behavior of the total $2\pi^0$ cross section has been assumed to be equal to the experimental one of $\pi^+\pi^-$ photoproduction multiplied by a scale factor equal to 0.4. The angular distribution of the two π^0 's has been calculated according to phase space. The double- π^0 contamination calculated in this way varies from 2 up to 6%, the highest value being reached for the measurement at $k_0 = 230$ MeV.

(c) *Nuclear absorption.* This can stop, in our telescope, energetic protons produced in the reaction $\gamma p \rightarrow p\pi^0$ by more energetic unpolarized photons. We have calculated the correction on the asymmetry values needed because of this effect, taking into account the whole flux of photoproduced protons through our telescope. The correction turns out to be less than 3%, except for the point measured at $k_0 = 230$ MeV, which is largely contaminated by protons coming from the resonance region (in this case this correction amounts to 15%). All the values of R_c and Σ reported in Table I have already been corrected for effects (b) and (c).

Other sources of systematic errors like liquid-hydrogen density variation and the stability of the beam monitor have not been considered.

We stress, that because the asymmetry measurement is a relative one, any counting loss due to counter inefficiency or proton-nuclear absorption does not affect the measured asymmetry value.

The error on the asymmetry has been calculated from the formula

$$\frac{\Delta\Sigma}{\Sigma} = \left[\frac{1}{N} \frac{1}{(\Sigma\bar{P})^2} + \left(\frac{\Delta\bar{P}}{\bar{P}} \right)^2 \right]^{1/2}. \quad (6)$$

The total number of events N and consequently the measurement time have been chosen to have almost the

same contributions to $\Delta\Sigma/\Sigma$ from the two terms appearing in the square root in Eq. (6). As previously mentioned, for the error on the polarization, we assumed $\Delta\bar{P}=0.01$.

The final values of the asymmetry are also shown in Fig. 6. The previous asymmetry measurements made by Drickey and Mozley^{5,24} are presented in the same figure.

The theoretical curves shown in Fig. 6 refer to the following calculations:

Curve (1)—Berends *et al.*⁶ The theoretical predictions are made on the basis of the dispersion relations. (The shadowed area reflects the uncertainty due to the approximations introduced in the calculations.) The ω exchange in the t channel is not considered. There are no free parameters in the theory.

Curve (2)—Rollnik *et al.*¹⁷ This calculation is also based on the dispersion theory. The ω (and also the ρ) exchange is introduced as a pole in the t channel. Three parameters have been introduced, and their values have been fixed by the authors from the fit of the angular distributions.

Curves (3) and (3')—Schwela.¹⁶ The calculation has been made by using dispersion relations. The ω contribution is not taken into account, but its relevance to the theory is discussed in this paper together with the uncertainty regarding the proper way to evaluate the ω exchange.

Curve (4)—Schmidt.¹² This curve is also calculated from dispersion-relation theory.

Curve (5)—Walker.¹⁹ This calculation is based on a phenomenological model in which the electric Born term is considered together with the resonances known from the pion-nucleon-scattering phase-shift analysis. A correction for the nonresonant part is introduced as a parameter with the restriction of smooth energy behavior.

From Fig. 6 we see that the curve in better agreement with the experimental results is curve (2). We recall that this is the only curve that explicitly takes into account vector-meson exchange. In fact, the authors introduced ω exchange and ρ exchange (this last one, however, should be less important) with the following coupling constants⁷:

$$g_{\omega\pi\gamma}/4\pi=0.15, \quad g_{\rho\pi\gamma}/4\pi=0.02,$$

²⁴ Of the four asymmetry values measured by the Stanford group, those at 285 and 435 MeV have been measured at a proton angle $\theta^*=90^\circ$ in the c.m. system. Those at 235 and 335 MeV have been done at $\theta^*=60^\circ$ and 120° , respectively. The corresponding values for the asymmetry at 90° have been obtained from the relationship $\Sigma(\theta^*)=\Sigma(90^\circ)\sin^2\theta^*[d\sigma(90^\circ)/d\sigma(\theta^*)]_{\text{unpol}}$, which is derived from Eq. (1), assuming that the coefficient $I(k,\theta^*)$ does not depend on θ^* . The ratio $[d\sigma(90^\circ)/d\sigma(\theta^*)]_{\text{unpol}}$ has been taken from the data of the Bonn group (Ref. 26).

which were taken from the quark model; and with

$$g_{\omega NN1^2}/4\pi=2.83, \quad g_{\rho NN1^2}/4\pi=0.86, \\ g_{\omega NN2^2}/4\pi=0.03, \quad g_{\rho NN2^2}/4\pi=9.66,$$

which were derived from nucleon-nucleon scattering.

The marked difference in Fig. 6 between curve (2) and the other ones in the low-energy region could then be due to ω exchange, whose importance would be confirmed by the asymmetry measurements. However, it is hard to understand what amount of this difference is due to ω exchange and what to the different methods employed in applying the dispersion relations to photoproduction; in fact, no author has published both the predictions (with or without ω exchange) of his theory on the asymmetry.

In order to get information on the multipole $E_{1+}^{(3)}$ at the resonance, we computed²⁵ the values of the asymmetry using the multipoles of BDW (the only ones available in numerical tables).

We found that the asymmetry is not very sensitive to the value of the leading multipole $M_{1+}^{(3)}$, while it is greatly influenced by $E_{1+}^{(3)}$. Our results are in much better agreement with $E_{1+}^{(3)}$ equal to zero than with $E_{1+}^{(3)}$ equal to the BDW estimate.

Meanwhile, we noticed that the BDW multipoles are not in good agreement with the recent measurements of the Bonn group²⁶ on the cross sections. These last ones seem to require^{27,28} (1) a position of the 33 resonance (at $k=349$ MeV according to BDW) shifted towards lower energies (this does not affect the asymmetry significantly); (2) a value of $M_{1+}^{(3)}$ a few percent higher; and (3) $E_{1+}^{(3)}$ different from zero.

In order to bring the BDW predictions in better agreement with both the asymmetry and cross-section measurements in addition to requirements (1) and (2), a value of $E_{1+}^{(3)}$ between zero and the BDW estimate would be required.

The $M_{1-}^{(0)}$ and $M_{1-}^{(1)}$ multipoles which concern the P_{11} resonance could be tentatively obtained from the relation (s - and p -wave approximation)

$$\frac{k}{q} \frac{d\sigma}{d\Omega}(90^\circ) \Sigma(90^\circ) |_{p\pi^0, p\pi^-} \\ = 3 \operatorname{Re}(E_{1+} - M_{1+})^* \left(\frac{3}{2} E_{1+} + \frac{1}{2} M_{1+} + M_{1-} \right) |_{p\pi^0, p\pi^-}$$

²⁵ We thank here M. Nigro, P. Spillantini, and V. Valente, who lent us a general program for calculating all photoproduction cross sections, asymmetries, and polarizations.

²⁶ G. Fischer *et al.*, University of Bonn Report No. 1-044, 1968 (unpublished).

²⁷ At the time of submission of this paper we received an unpublished report from the Orsay group (Ref. 28) reporting measurements of the angular distributions for π^0 photoproduction at the first pion nucleon resonance. Their results seem to confirm the behavior of the cross sections measured by the Bonn group, but are slightly smaller (up to 5-7% at $\theta^*=90^\circ$). This leaves substantially unaffected our conclusions drawn from the simultaneous analysis of angular distributions and asymmetry measurements.

²⁸ R. Morand, E. F. Erickson, J. P. Pahin, and M. G. Crossiaux, Phys. Rev. **180**, 1299 (1969).

by putting in the first member the experimental results on reaction $\gamma p \rightarrow p\pi^0$ and $\gamma n \rightarrow p\pi^-$, and in the second member the BDW multipoles, leaving only $\text{Re}M_1^{(0)}$ and $\text{Re}M_1^{(1)}$ to be determined. However, this analysis is not free of ambiguities for the following two reasons: (1) The BDW multipoles are not in good agreement with the Bonn results on $d\sigma/d\Omega$, as previously mentioned; (2) There is a big cancellation when performing the sum $M_1^{(0)} + \frac{1}{2}M_1^{(1)}$ because of the isospin decomposition (4) in the π^0 case. This fact makes it very hard to detect P_{11} effect in π^0 photoproduction.

ACKNOWLEDGMENTS

The theoretical introduction of this paper has been written with the critical advice of Dr. D. Weaver. We are very grateful to Dr. Weaver also for many stimulating suggestions and discussions clarifying the interpretation of our data. Thanks are also due to G. Di Stefano and co-workers for their skilled technical work. Finally, we would like to mention that the synchrotron staff collaborated very helpfully with us in providing smooth machine operation.

Scattering of Antineutrons by Protons*

A. D. FRANKLIN AND R. R. SOCASH
University of Colorado, Boulder, Colorado 80302
 (Received 4 March 1969)

The total and elastic cross sections for antineutrons on protons have been measured for antineutron momenta from 0.5 to 2.5 GeV/c. The results are in agreement with previous $\bar{p}p$ data at these momenta.

THE scattering of antineutrons by protons has been investigated using antineutrons obtained from a previously analyzed¹ sample of 841 events fitting the hypothesis



from a 2.7-GeV/c exposure in the Brookhaven 20-in. hydrogen bubble chamber. The momentum spectrum and effective pathlength of the antineutrons are shown in Fig. 1. The values of antineutron momentum ranged

from approximately 0.3 GeV/c to 2.5 GeV/c and peaked near 2.2 GeV/c.

For each event satisfying reaction (1), a three-view scan was done by two physicists to search for possible interactions along the computed antineutron direction. All interactions within a 5° half-angle cone of the computed antineutron direction were accepted for measurement. No minimum-tracklength criterion was applied during scanning. A total of 277 events were found which had at least one possible antineutron interaction. Each event including the recoil track(s) was measured in three views and processed through TVGP and SQUAW.

A total of 54 events fitted the three-constraint hypothesis to $\bar{p}p \rightarrow \bar{n}p\pi^-$ with a χ^2 probability greater than 1%. In these fits, the antineutron was constrained to pass through the proposed point of interaction. The momentum distribution of these events is shown by the shaded area in Fig. 1. The breakdown of the 54 events includes 36 single recoil tracks, 11 three-prong stars, and 7 five-prong stars. Fits to the various possible final states were tried and the results of these fits are given in Table I. Unique ionization-consistent fits to the $\bar{n}p$ interaction were made for 45 of the events.

The antineutron pathlength was calculated by computing the distance from the antineutron production vertex to the visible edge of the chamber for each event satisfying reaction (1). Corrections were made for the antineutrons which interacted before reaching the visible edge of the chamber. It was found that 19 of the 277 measured events which originally fitted reaction (1) when analyzed by DATPRO-GUTS did not give a fit with probability greater than 1% when analyzed by TVGP-

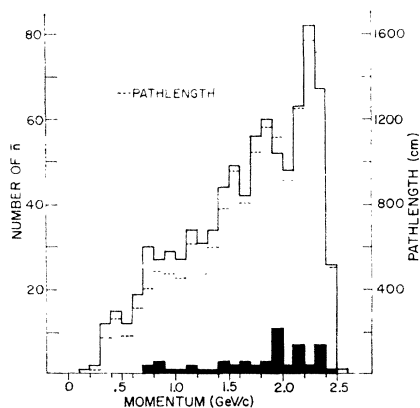


FIG. 1. The solid curve is the momentum spectrum for antineutrons from $\bar{p}p \rightarrow \bar{n}p\pi^-$. The dashed lines indicate the effective pathlength. Events which fit a three-constraint hypothesis are shown by the shaded area.

* Work supported by the U. S. Atomic Energy Commission under Contract No. AT(11-1)-1537.

¹ R. Sears, L. M. Libby, and R. R. Socash, Phys. Letters (to be published); R. Sears, Ph.D. thesis, University of Colorado (unpublished).